Journal of Catalysis 276 (2010) 292–305

Contents lists available at ScienceDirect

Journal of Catalysis

journal homepage: www.elsevier.com/locate/jcat

Support effects in the Au-catalyzed CO oxidation – Correlation between activity, oxygen storage capacity, and support reducibility

D. Widmann [a], Y. Liu [b], F. Schüth [b], R.J. Behm [a,*]

[a] Institute of Surface Chemistry and Catalysis, Ulm University, D-89069 Ulm, Germany
[b] Max-Planck-Institut für Kohlenforschung, D-45470 Mülheim an der Ruhr, Germany

ARTICLE INFO

Article history:
Received 13 July 2010
Revised 21 September 2010
Accepted 22 September 2010
Available online 9 November 2010

Keywords:
Au catalysts
CO oxidation
Support effects
Oxygen storage capacity (OSC)
Reaction mechanism

ABSTRACT

The oxygen storage capacity (OSC) and its correlation with the activity for the CO oxidation reaction and the reducibility of the support material were investigated for four different metal oxide-supported Au catalysts with similar Au loading and Au particle sizes (Au/Al_2O_3, Au/TiO_2, Au/ZnO, Au/ZrO_2), which were prepared by deposition of pre-formed Au colloids. Temporal Analysis of Products (TAP) reactor measurements show that the OSC and the activity for CO oxidation, measured under identical conditions, differ significantly for these catalysts and are correlated with each other and with the reducibility of the respective support material, pointing to a distinct support effect and a direct participation of the support in the reaction. Activity measurements performed under ambient conditions show a similar trend of the activity as the TAP reactor measurements, supporting that the conclusions drawn from the TAP reactor measurements are valid also under continuous reaction conditions. Moreover, the rapid formation and accumulation of carbon-containing surface species during reaction is demonstrated, which can severely reduce the activity for CO oxidation. Implications of these results on the CO oxidation mechanism over metal oxide-supported catalysts are discussed.

1. Introduction

Oxide-supported small Au nanoparticles have attracted considerable attention in recent years due to their high activity for catalyzing various oxidation and reduction reactions already at low temperatures [1]. Most prominent examples are the CO oxidation reaction [2–5], the water–gas shift reaction [6–9], or the selective and total oxidation of hydrocarbons [10–12]. Despite extensive studies, the physical origin of the high activity of supported Au catalysts and the underlying reaction mechanisms are still under debate [13,14]. Open questions are for example (i) the pronounced role of the Au particle size [15], which was explained, e.g., by quantum size effects [16] or a high activity of under-coordinated Au atoms at corners and edges [17–23], (ii) the nature of the active Au species (metallic Au nanoparticles or ionic/partly charged Au^{n+} or $Au^{\delta-}$ species) [24–28], (iii) the influence of the support material on the catalytic performance of the corresponding Au catalysts and its role in the reaction process [28–33], and in particular (iv) the activation of oxygen and the active site for oxygen activation [33–35]. The latter two questions are topic of the present study. They are approached in a simple way, by investigating the oxygen storage capacity (OSC) and its correlation with the CO oxidation activity of four different Au catalysts (Au/Al_2O_3, Au/TiO_2, Au/ZnO, Au/ZrO_2) with similar Au particle sizes and Au loadings, but with support materials which differ strongly in their reducibility. The catalysts were prepared by deposition of preformed Au nanoparticles ('colloidal deposition').

Based on numerous studies, there is no doubt that the support has a pronounced effect on the activity of these catalysts. Open and not yet resolved is the exact nature of this effect. Testing a variety of Au catalyst supported on different metal oxides for their activity in the CO oxidation reaction, Schubert et al. [29] distinguished between two major groups of support materials, reducible materials leading to 'active' catalysts and non-reducible materials resulting in 'inactive' (or little active) catalysts. The difference was tentatively attributed to the different ability of these materials to create oxygen vacancies on the support, close to the Au particles, which were proposed as active centers for oxygen activation during the CO oxidation reaction. However, there are a number of different possibilities for the support to modify the activity of the catalyst. In addition to directly participating in the reaction, the support may affect the reaction also indirectly, by influencing the shape and size of the Au nanoparticles during the catalyst preparation and activation procedure, via metal–support interactions [22], by support-induced strain in the Au nanoparticles [18], by charge transfer from or to the Au nanoparticles [36] or by stabilizing ionic Au species [37].

* Corresponding author. Fax: +49 731 50 25452.
E-mail address: juergen.behm@uni-ulm.de (R.J. Behm).

0021-9517/$ - see front matter © 2010 Elsevier Inc. All rights reserved.
doi:10.1016/j.jcat.2010.09.023

Several groups have tried to discriminate between these possibilities by producing Au catalysts with similar Au loading and particle size, either by traditional routes, e.g., by deposition–precipitation techniques [22,28], or by depositing pre-formed Au nanoparticles of similar size on different support materials [38–40] and comparing their activity. In a careful TEM study, Janssens et al. compared Au catalysts supported on TiO_2, $MgAl_2O_4$, and Al_2O_3 and arrived at the conclusion, that the differences in reactivity of these catalysts can mainly be explained by the different numbers of under-coordinated Au sites on the Au nanoparticles [22], although other support-induced effects have to be considered as well to understand the lower activity of the Au/Al_2O_3 catalyst. Comparing the reduction behavior of Au^{3+} species and the CO oxidation activity of Au/TiO_2, Au/CeO_2, and Au/Al_2O_3 catalysts, which were prepared by a deposition–precipitation procedure and subsequent activation, Delannoy et al. noted that both properties are strongly affected by the support and that the CO oxidation activity of these catalysts is related to the presence of Au^0 nanoparticles. On the reduced catalysts, the activity was found to decrease in the order $Au/TiO_2 \approx Au/CeO_2 \gg Au/Al_2O_3$ [28]. To minimize effects caused by support-dependent differences in the Au^{3+} reduction behavior, Comotti el al. performed a similar comparison of the CO oxidation activity using Au catalysts (Au/Al_2O_3, Au/TiO_2, Au/ZnO, and Au/ZrO_2) with similar Au loadings and particle size distributions, which were prepared via a colloidal deposition method [40]. Also these authors found that the nature of the support has a significant influence on the catalytic properties. This influence, however, did not follow the reducibility of the supports. They tentatively suggested that support-induced variations in the shape of the Au nanoparticles, due to metal–support interactions, lead to faceting and defect sites and this way affect the activity. Similar studies were performed also by Grunwaldt et al. [17] and Arrii et al. [39]. Also in these studies, the activity of the catalysts depended strongly on the nature of the metal oxide used as support material; the origin of the different catalytic performance of the corresponding Au catalysts, however, remained controversial. Recent TAP reactor measurements have shown that Au/TiO_2 and $AuCeO_2$ catalysts are able to reversibly store and release active oxygen on the surface upon adsorption from O_2 or reaction with CO, respectively [33,41,42]. This active oxygen was stable against desorption at least up to 120 °C. Furthermore, for Au/TiO_2 catalysts with different particle sizes but similar Au loading, the OSC and the activity for CO oxidation were found to be closely correlated and to scale with the perimeter of the interface between Au nanoparticles and TiO_2 support, pointing to a direct involvement of these interface sites as active sites for oxygen storage and in the CO oxidation reaction [33].

In the present study, we will apply Temporal Analysis of Products (TAP) reactor measurements, which allow us to directly determine the OSC of the different catalysts and thus to reveal possible correlations between OSC, CO oxidation activity, and redox behavior of the different support materials. From these results, we can derive a direct participation of the support in the CO oxidation reaction, which has not been possible by any other technique up to now. Following a brief description of the experimental set-up and procedures, we will first present results characterizing the physical properties of the catalysts such as the loading and size of the Au nanoparticles and the surface area of the different catalysts (Section 3.1), followed by measurements of the CO oxidation kinetics under atmospheric pressure (Section 3.2), and finally the results of the TAP reactor measurements (Section 3.3). The latter included both multi-pulse sequences for determining the OSC and single-pulse measurements, with simultaneous pulses of CO and O_2, for evaluation of the CO oxidation activity under these conditions. In addition, changes of the oxidation state during reaction (differences in CO consumption and O_2 consumption) and the build-up of carbon-containing surface species (differences in CO consumption and CO_2 formation) on the different catalysts are evaluated. Finally, the stability and dynamic behavior of the carbon-containing surface species is evaluated in transient experiments using isotope labeling techniques. Consequences of these data on the CO oxidation mechanism will be discussed.

2. Experimental

2.1. Catalyst preparation

The four different Au catalysts were prepared by a colloidal deposition method using commercial, non-porous metal oxides. This method was described in detail in Refs. [43,44]. First, colloidal Au solutions were prepared by adding polyvinyl alcohol (PVA) as protecting agent to an aqueous solution of gold acid ($HAuCl_4$) at room temperature. Afterward, gold reduction was initiated by rapid injection of an aqueous solution of $NaBH_4$, resulting in an orange-brown gold sol with metallic Au particles. To this gold sol, the support material was added under stirring, which was continued until all of the Au particles were adsorbed on the surface (nominal loading 1 wt.%). Similar to the work of Comotti et al. [40], we used the following support materials: P25 from Degussa for the Au/TiO_2 catalyst, AC-45 from Brüggemann Chemicals for the Au/ZnO catalyst, PURALOX SBa-200 from Sasol for the Au/Al_2O_3 catalyst, and $Zr(OH)_4$ from MEL Chemicals for the Au/ZrO_2 catalyst. While the first three supports were used as received, the latter one was additionally calcined at 350 °C for 4 h prior to the Au deposition in order to obtain dehydroxylated ZrO_2. The resulting raw catalysts were washed and dried under vacuum (10^{-2} mbar) in a desiccator with P_2O_5 as drying agent and then stored in the desiccator until use. Catalyst preparation and storage took place under exclusion of light.

Prior to all measurements, the catalyst was first dried for 1000 min in order to obtain the same water content on all samples, independent of the previous history (TAP reactor: vacuum drying at room temperature; plug-flow reactor: drying in a flow of 20 Nml min^{-1} N_2 at 100 °C) and afterward calcined in a flow of 20 Nml min^{-1} 10% O_2/N_2 at 250 °C for 2 h in order to remove the protecting agent (henceforth this procedure will be denoted as "O250"). For heating and cooling, the temperature was raised/decreased by 10 °C min^{-1} in a flow of 20 Nml min^{-1} Ar (TAP reactor) or N_2 (plug-flow reactor). For calcination as well as for reaction measurements (described below), high purity gases from Westphalen were used as delivered (CO 4.7, O_2 5.0, N_2 6.0, and Ar 6.0).

2.2. Catalyst characterization

The surface area of the catalysts was determined by low-temperature nitrogen adsorption using the method of Brunauer, Emmet, and Teller (BET) for evaluation. The Au content of the raw catalysts was measured by inductively coupled plasma optical emission spectrometry (ICP-OES), and the Au particle size was evaluated from transmission electron microscopy (TEM) images.

2.3. Catalytic activities

First, the catalytic activity for CO oxidation on the four catalysts was evaluated in a conventional micro-reactor at atmospheric pressure (120 °C reaction temperature, 1000 min reaction time) after *in situ* calcination (O250, description see above). The catalysts were diluted with α-Al_2O_3 in order to obtain differential reaction conditions. Depending on the activity of the respective catalyst, it was 1:120 for Au/TiO_2, 1:10 for Au/ZnO, and 1:5 for Au/ZrO_2; no dilution was used for Au/Al_2O_3. This resulted in conversions of

below 15% for CO and O_2 during the activity measurements. About 65 mg of the diluted catalysts were placed in the center of a quartz tube micro-reactor (i.d. 4 mm). The gas flow was 60 Nml min^{-1} (1 kPa CO, 1 kPa O_2, rest N_2); influent and effluent gases were analyzed by on-line gas chromatography (DANI, GC 86.10). For further details on the set-up and the evaluation procedure, see Ref. [45].

2.4. Pulse experiments

The pulse experiments were performed in a home-built TAP reactor which was described in detail in Ref. [46]. It is comparable to a design published by Gleaves et al. (TAP-2) [47], easy to operate and excels by its highly reproducible pulse sequences. It consists of a gas mixing unit, two independently working piezo-electrically driven pulse valves and a tubular quartz glass micro-reactor (90 mm long, 4 mm i.d., 6 mm o.d.), which was heated by a ceramic tube furnace and connected to an ultra high vacuum system (analysis chamber). Pulses of typically 1×10^{16} molecules, generated by piezo-electric pulse valves, were directed into the micro-reactor. Exact numbers of the amount of molecules admitted per pulse were calculated by comparison with the signal of the internal standard argon, which was included in every pulse. In the central part of the reactor, the catalyst bed was fixed by two stainless steel sieves (Haver & Boecker OHG; aperture 25 μm, transmission 25%). The catalyst bed itself consisted of three zones: the catalyst zone containing the catalyst diluted with SiO_2 in the center ('reaction zone') and two additional zones with inert material before and after the catalyst zone ('gebaflot 010' from Dorfner GmbH; grain size 100–200 μm) acting as diffusion zones [48]. The stainless steel sieves as well as the quartz powder were tested to be inactive for the CO oxidation in the temperature range investigated. The amount of catalyst and the dilution were different for different types of experiments and are described below. After passing through the reactor, the gases were analyzed by a quadrupole mass spectrometer (QMG 700, Pfeiffer Vacuum) located in the analysis chamber closely behind the reactor tube. The consumption of CO and O_2 in the respective pulses was calculated from the missing mass spectrometric intensity in these pulses compared to the intensity after saturation. The formation of CO_2 was determined directly from the CO_2 pulse intensity. For *in situ* conditioning of the catalyst at atmospheric pressure prior to the measurements, the reactor can be separated from the UHV system by a differentially pumped gate valve and connected directly to an adjustable roughing pump [46].

In the multi-pulse experiments, the catalysts were exposed first to a sequence of 200 CO/Ar and then to a sequence of 100 O_2/Ar pulses, in order to reactively remove and deposit active oxygen. In these experiments, we used 10 mg of each catalyst diluted with SiO_2 in a ratio 1:2, and the content of Ar molecules was 50% in each pulse.

For evaluating the catalytic activity in the TAP reactor, the samples were exposed to CO and O_2 at the same time by simultaneous CO/Ar and O_2/Ar pulses (with 50% Ar each) ('single-pulse' measurements). The resulting CO:O_2 ratio was 1:1. Hence, there was an excess of oxygen compared to the stoichiometry of the CO oxidation reaction. These measurements were used to compare the catalytic activity of the four differently supported Au catalysts. Therefore, the amount of catalyst (5 mg) and the dilution with SiO_2 (1:5) were identical for all of these measurements. Additional, single-pulse experiments using labeled ^{13}CO were performed, which aimed at evaluating the stability of adsorbed carbon-containing species under reaction conditions. Here, first a reaction mixture containing labeled ^{13}CO was pulsed with one pulse valve (45% ^{13}CO, 45% O_2, 10% Ar), followed by pulses containing non-labeled ^{12}CO with the other pulse valve (45% ^{12}CO, 45% O_2, 10% Ar). Here, the amount of catalyst and the dilution were slightly different than in the simultaneous-pulse measurements (Au/TiO_2: 10 mg, Au/ZrO_2: 3 mg, Au/ZnO: 5 mg, Au/Al_2O_3: not measured).

2.5. Temperature-programmed desorption

To identify carbon-containing adsorbed species, which were accumulated on the catalyst surface during reaction, we also performed temperature-programmed desorption (TPD) measurements in the TAP reactor. The measurements started 5 min after finishing the reaction, heating the catalyst from reaction temperature (120 °C) to 800 °C (25 °C min^{-1}) without an additional carrier gas. The effluent gases arising from decomposition/desorption of the surface species were detected by the mass spectrometer.

3. Results and discussion

3.1. Catalyst characterization

3.1.1. Au content

The Au content of the Au catalysts was determined by inductively coupled plasma-optical emission spectroscopy (ICP-OES), measured two times by repeat determination. For the Au/TiO_2, Au/ZrO_2, and Au/ZnO catalysts, it was 1.0 wt.%, identical to the nominal loading obtained upon complete deposition of the Au particles on the support. Only for the Au/Al_2O_3 catalyst, the Au content was slightly lower (0.8 wt.%) (see Table 1). This catalyst required also the longest time (24 h) for depositing the Au nanoparticles. For comparison, on the TiO_2 support, where the deposition was fastest, it took only 30 min to adsorb all Au nanoparticles and reach the nominal Au loading of 1.0 wt.%.

3.1.2. Au particle size

The Au particle sizes on the various catalysts were measured by transmission electron microscopy (TEM). Representative images for each catalyst are shown in Fig. 1. In these images, the dark spots represent the Au particles. The evaluation of >100 particles for each catalyst resulted in mean Au diameters of 3.3 ± 1.0 nm for Au/TiO_2, 2.4 ± 0.7 nm for Au/ZrO_2, 3.1 ± 0.9 nm for Au/ZnO, and 3.5 ± 1.1 nm for Au/Al_2O_3. The corresponding particle size distributions are shown in Fig. 2. Assuming half-spherical Au particles and 1.15×10^{15} Au atoms cm^{-2}, we can further calculate the dispersion of each catalyst, which is listed in Table 1. It should be noted that for similar catalysts Comotti et al. found Au particle sizes which are slightly (0.3 nm) smaller than in the present study, which can be explained by the different pre-treatment (pre-treatment in reaction atmosphere vs. O250) [40].

3.1.3. Surface area

The surface areas of all four catalysts, as measured by low-temperature nitrogen adsorption (BET), were close to the surface areas of the corresponding support materials. They are 198 $m^2\ g_{cat}^{-1}$ for the Au/Al_2O_3 catalyst, 47 $m^2\ g_{cat}^{-1}$ for the Au/TiO_2 catalyst,

Table 1
Physical properties of the different supported Au/M_xO_y catalysts after pre-treatment by calcination in 10% O_2/N_2 at 250 °C for 2 h (O250).

	Au/TiO_2	Au/ZrO_2	Au/ZnO	Au/Al_2O_3
Au loading[a] (wt.%)	1.0	1.0	1.0	0.8
Au diameter[b] (nm)	3.3 ± 1.0	2.4 ± 0.7	3.1 ± 0.9	3.5 ± 1.1
Surface area[c] ($m^2\ g_{cat}^{-1}$)	47	201	50	198
Dispersion (%)[d]	30	42.	33	28

[a] Measured by ICP-OES.
[b] Measured by TEM.
[c] Measured by low-temperature N_2 adsorption (BET).
[d] Assuming half-spherical Au particles.

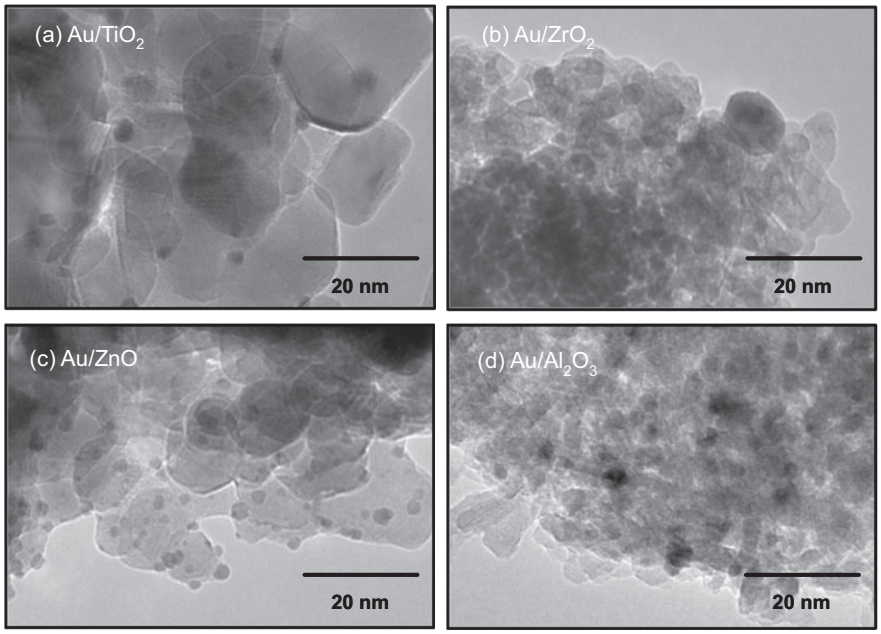

Fig. 1. Representative TEM images of the four differently supported Au catalysts after calcination in 10% O_2/N_2 at 250 °C for 2 h (O250).

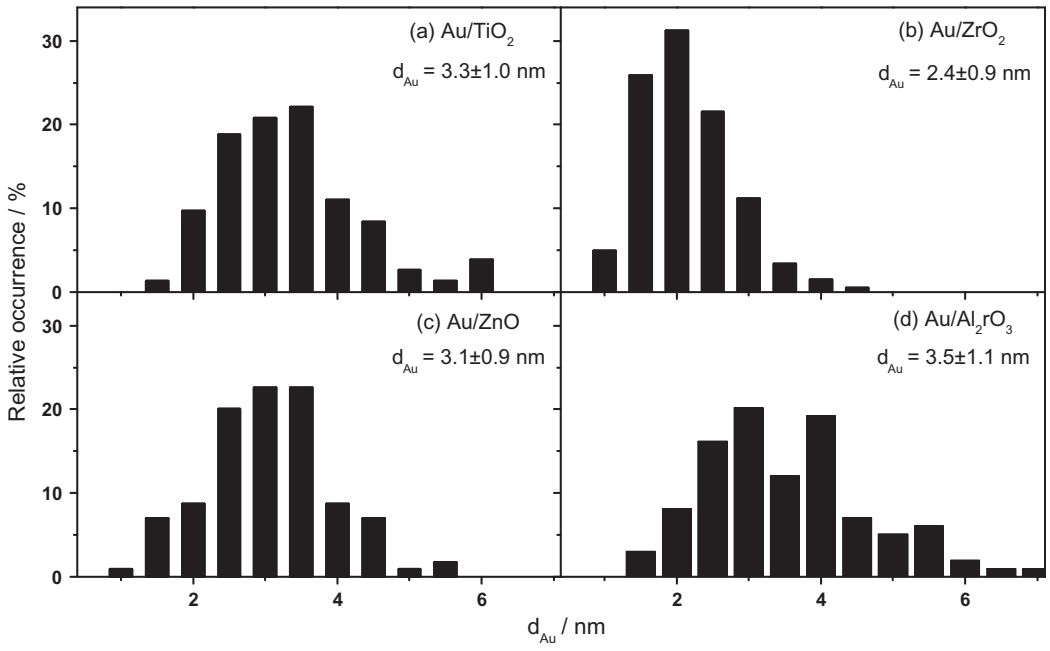

Fig. 2. Particles size distributions of the (a) Au/TiO_2, (b) Au/ZrO_2, (c) Au/ZnO, and (d) Au/Al_2O_3 catalysts after calcination in 10% O_2/N_2 at 250 °C for 2 h (O250).

50 $m^2\ g_{cat}^{-1}$ for the Au/ZnO catalyst, and 201 $m^2\ g_{cat}^{-1}$ for the Au/ZrO_2 catalyst (see also Table 1).

3.2. Kinetic measurements

Fig. 3 shows the Au mass normalized reaction rates measured for the CO oxidation reaction over the four different supported catalysts under differential reaction conditions. Because of the similar Au loadings and mean Au particle sizes of the four catalysts, these reaction rates are a direct measure for the inherent catalytic activity of the respective catalysts. The reaction rates obtained under steady-state conditions, after 1000 min time on stream, are 1.1×10^{-2}, 7.7×10^{-4}, 4.1×10^{-4}, and 7.1×10^{-5} mol $s^{-1}\ g_{Au}^{-1}$ for Au/TiO_2, Au/ZrO_2, Au/ZnO, and for Au/Al_2O_3, respectively (see also Table 2). The corresponding TOF numbers, which decrease in the same order due to the almost identical Au particle sizes, are 7.1, 0.37, 0.24, and 0.05 s^{-1}, respectively. The pronounced differences in activity for CO oxidation, which differed by almost a factor of 200 between the most active (Au/TiO_2) and the least active (Au/Al_2O_3) catalyst, despite of comparable Au nanoparticle sizes, are clear evidence for a distinct effect of the support on the catalytic activity of the corresponding catalysts. This will be discussed in detail later.

These results can be compared with data on the catalytic activities of the very same Au catalysts published recently [40], where the temperature needed for 50% conversion of CO (T_{50}) was used

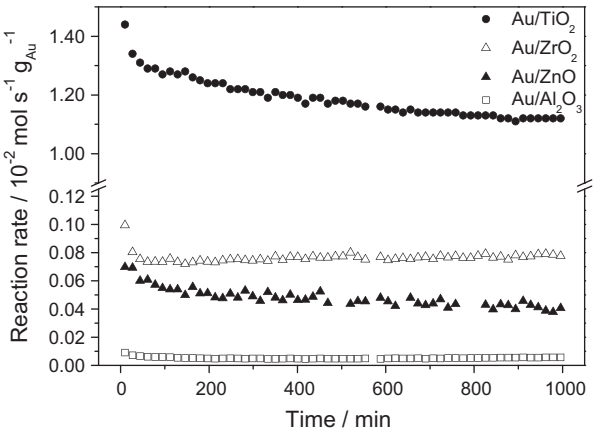

Fig. 3. Au mass normalized reaction rates during the CO oxidation at 120 °C over the four differently supported Au catalysts after calcination in 10% O_2/N_2 at 250 °C for 2 h (O250) (1 kPa CO, 1 kPa O_2, and balance N_2).

as measure for the activity (reaction atmosphere: 1 kPa CO, 20 kPa O_2, rest N_2). The T_{50} temperature varied from $T_{50} = -14$ °C for Au/TiO_2, closely followed by Au/Al_2O_3 (values between −12 and 46 °C), to $T_{50} = 50$ °C for Au/ZnO and $T_{50} = 74$ °C for the least active the Au/ZrO_2 catalyst [40]. Based on these data, Comotti et al. suggested that the reducibility of the support is not the decisive factor for CO oxidation activity. Qualitatively, our results agree reasonably well with those findings, except for the Au/Al_2O_3 catalyst, which had an outstandingly high activity in that earlier study, with a T_{50} value comparable to that of the Au/TiO_2 catalyst, while in the present study its activity was distinctly lower than that of all other catalysts. Slight differences in the pre-treatment procedures (activation during reaction in the first study and O250 pre-treatment in the present study) and in the reaction conditions (lower oxygen concentration and differential reaction conditions in the present study) may explain the reversed order in the catalytic activities of Au/ZnO and Au/ZrO_2, but cannot explain the large difference in activities measured for the Au/Al_2O_3 catalyst in the two studies. The low activity of the Au/Al_2O_3 catalyst was reproduced for several batches synthesized independently, and also under conditions comparable to those being used in the above-mentioned study.

The results obtained over the different supported catalysts agree perfectly with the trends proposed by Schubert et al., who distinguished between 'active' and 'inert' support materials depending on their reducibility, with the inert materials being not or hardly reducible [29]. They came to the conclusion that the active supports participate in the catalytic process, most likely by the adsorption and activation of oxygen at oxygen vacancies on the support material close to the Au particles or at the interface between Au particles and support. On a molecular scale, this would be attributed to the ability of the support to store and/or activate oxygen and release it for the oxidation of CO, which is generally agreed to adsorb on the Au nanoparticles [1,13,34,49,50]. Grunwaldt et al. compared the CO oxidation activity of Au catalysts supported on two different metal oxides (Au/TiO_2 and Au/ZrO) [17], using pre-formed, 'size-controlled' Au particles deposited on the different supports, similar to the present work, and a similar study was reported by Arrii et al. [39], investigating CO oxidation on Au/TiO_2, Au/ZrO_2, and Au/Al_2O_3 catalysts. Comparable to the results of Schubert et al., these authors found the catalytic activity for CO oxidation to decrease with decreasing reducibility of the support material (Au/TiO_2 > Au/ZrO_2 ≫ Au/Al_2O_3). Grunwaldt et al. explained the differences in catalytic activity by different shapes of the Au nanoparticles deposited on different supports, as evidenced by DRIFTS (CO adsorption) and TEM measurements, while Arri et al. suggested a synergetic or cooperative effect between the TiO_2 or ZrO_2 support and the Au nanoparticles for the active Au/TiO_2 and Au/ZrO_2 catalysts, with the support participating in the reaction [39]. On the other hand, in apparent disagreement to this proposal and the results presented here, some groups also reported high activities for Au catalysts supported on "inert" metal oxides such as Au/Al_2O_3, showing activities close to or even superior to Au/TiO_2 [51,52]. In the study by Wolf et al., however, the Au particle size was lower for the catalysts supported on the inert metal oxide (Au/Al_2O_3) than for the Au/TiO_2 catalyst used for comparison. When comparing catalysts with the same Au particle size on Al_2O_3 and TiO_2, the Au/Al_2O_3 catalyst is significantly less active for CO oxidation than the Au/TiO_2 catalyst also in that study [51]. Nevertheless, in all of these studies, possible effects of the support on the catalytic activity have been somehow tentative, since a direct participation of the support under relevant reaction conditions was not investigated. This will be topic of the following chapter, where we compare the differently supported catalysts in terms of their ability to form active oxygen on the surface.

3.3. Pulse experiments

Possible relationships between activity and reducibility of the different catalysts were tested by pulse experiments in a TAP reactor, which allow us to quantify the amount of the active oxygen (OSC) stored under reduced pressure conditions [33,41,42] (Section 3.3.1). Moreover, the catalytic activity for CO oxidation was tested also under the same conditions as used in the OSC measurements (Section 3.3.2).

3.3.1. Oxygen storage capacity

The oxygen storage capacity of all four catalysts was measured at 120 °C reaction temperature in multi-pulse experiments,

Table 2
Oxygen storage capacity (OSC), catalytic activity for CO oxidation, and amount of carbon-containing surface species accumulated on the surface during reaction at 120 °C on the differently supported Au catalysts after calcination (O250).

	Au/TiO_2	Au/ZrO_2	Au/ZnO	Au/Al_2O_3
OSC (10^{18} O atoms g_{cat}^{-1})	1.5	1.2	0.9	<0.1
Additional amount of active oxygen present after O250 calcination relative to re-oxidation by O_2 pulsing (10^{18} O atoms g_{cat}^{-1})	1.2	1.1	3.2	–
Additional amount of active oxygen present after O250 calcination relative to steady-state during single-pulse measurements (10^{18} O atoms g_{cat}^{-1})	1.1	1.0	4.0	–
Reaction rate (plug-flow reactor) (mol g_{cat}^{-1} s^{-1})	1.1×10^{-4}	7.7×10^{-6}	4.1×10^{-6}	5.7×10^{-7}
Reaction rate (plug-flow reactor) (mol g_{Au}^{-1} s^{-1})	1.1×10^{-2}	7.7×10^{-4}	4.1×10^{-4}	7.1×10^{-5}
TOF (plug-flow reactor) (s^{-1})	7.1	0.37	0.24	0.05
Relative CO conversion under steady-state conditions (TAP reactor)	53%	28%	11%	<2%
Carbon-containing surface species under steady-state conditions (TAP reactor) (10^{18} molecules CO_2 g_{cat}^{-1})	<0.2	7.7.	2.7	<0.2

exposing the O250 pre-treated catalysts alternately to sequences of 200 CO/Ar pulses and 100 O_2/Ar pulses, starting with the CO/Ar pulses. It was ensured that after these numbers of pulses there is no further uptake of CO or O_2, i.e., further reduction or oxidation of the corresponding catalysts was below the detection limit under these conditions. This reduction–oxidation cycle was repeated at least three times on each catalyst for determining the amount of active oxygen which is reversibly stored on the catalyst surface, i.e., which can be removed by reaction with CO during CO pulses and re-deposited by O_2 pulses. The corresponding mass spectrometric signals recorded over the different catalysts during these measurements are reproduced in Fig. 4, which shows pulses of the reactants CO/Ar and O_2/Ar, respectively, and of the CO_2 signal obtained during the CO pulses. Since the uptake of CO and O_2, which is indicated by the missing intensity in the pulse response, is biggest at the beginning of each pulse sequence, only the first 20 pulses of CO/Ar (out of 200 pulses) or O_2/Ar (out of 100 pulses) are shown here. (It should be noted that in all sequences, the first pulse is somewhat lower in intensity than the subsequent ones. For quantitative evaluation, this is corrected for by comparison with the internal Ar standard.) The qualitative behavior for CO consumption and for oxygen consumption is similar for all samples: at the beginning of each pulse sequence, there is almost 100% conversion of CO and O_2. Afterward, the consumption of the respective reactants decreases with ongoing change of the catalyst oxidation state, until there is no more uptake or conversion of reactant detected. At this point, the catalyst has reached a state which we define as its fully re-oxidized or reduced state, respectively. The consumption in CO and O_2 at the beginning of each sequence is clear evidence for the ability of the catalyst to store oxygen upon O_2 exposure and to remove it by reaction with CO. While being reactive toward CO, this oxygen species is stable against desorption on these catalysts. It should be stressed that from these data alone we cannot conclude on the nature of the active oxygen species; in particular, we cannot decide whether this is an atomic or molecular oxygen species.

For CO_2, the results differ considerably, depending on the support used. In general, CO_2 formation is detected only during CO pulses, but the shape and intensity of the CO_2 signals varied considerably. For the Au/TiO_2 catalyst, we obtained distinct and sharp pulse responses, while for the Au/ZnO catalyst the signals are very broad. For the Au/Al_2O_3 catalyst, the CO_2 signals are much less intense and close to the background signal, and for the Au/ZrO_2 catalyst, a quantitative evaluation was no more possible since the signals were essentially buried in the noise of the background intensity. Since there is obviously consumption of CO during the pulse sequence with the CO/Ar mixture, we expect also for this catalyst the formation of CO_2, due to the reaction of CO with surface oxygen. The absence of a CO_2 signal is explained by a rather strong effective interaction between CO or CO_2 and the ZrO_2 support, which leads to an accumulation of carbon-containing species on the surface or at least to a very prolonged pulse response that cannot be resolved any more. These data illustrate the differences in the effective interaction strength between CO_2 and the different supports, which is lowest for Au/TiO_2 and distinctly higher for the Au/ZnO and Au/ZrO_2 catalysts (further discussion see Section 3.3).

The accumulated, absolute amounts of CO molecules converted or O_2 molecules adsorbed during the multi-pulse experiments over the different Au catalysts are plotted in Fig. 5. For all catalysts, the overall uptake and conversion of CO was higher during the first sequence of CO/Ar pulses, which was dosed on a freshly calcined catalyst, than in the following sequences. Hence, on all catalysts, thermal oxidation of the catalyst in a O_2/N_2 flow at 250 °C and atmospheric pressure results in a higher amount of active oxygen stored on the catalyst surface than can be obtained upon re-oxidation by O_2 pulses. Similar observations were made by Kotobuki et al. [33] and by Tost et al. [42] during identical measurements

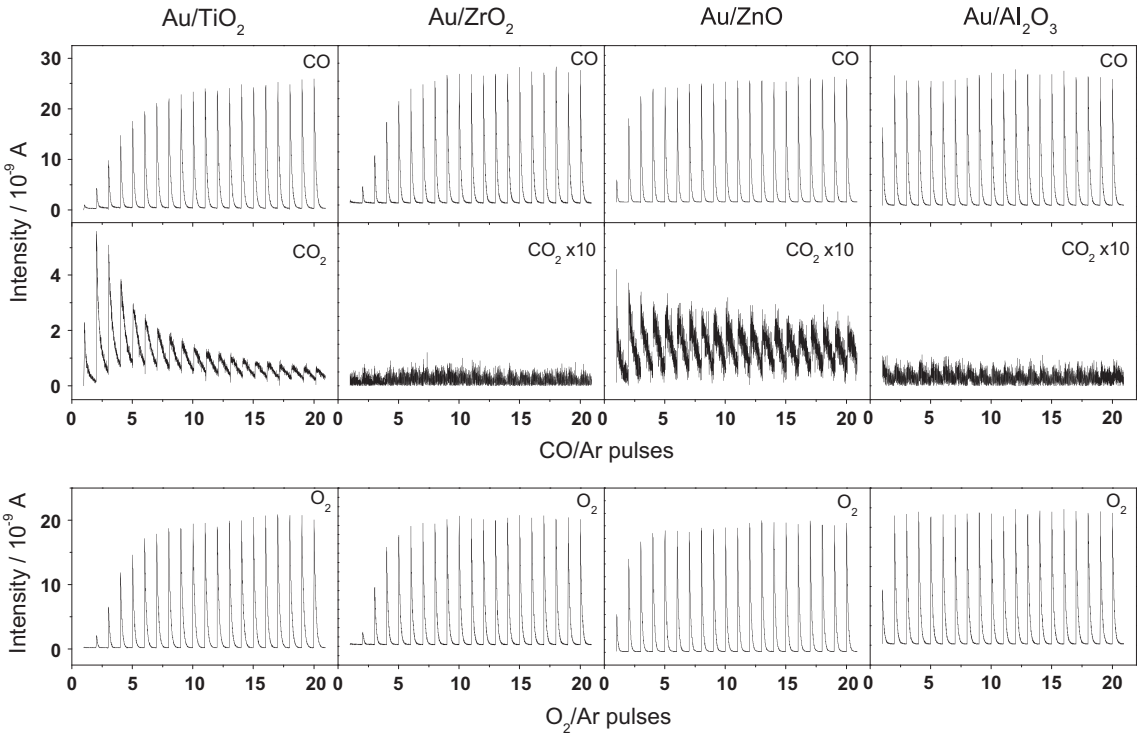

Fig. 4. Pulse responses during the multi-pulse experiments at 120 °C on the four differently supported Au catalysts after calcination (10% O_2/N_2, 250 °C, 2 h – O250) for determination of the oxygen storage capacity. Since the changes are biggest at the beginning of each sequence, only the first 20 pulses each of CO/Ar pulses (out of 200) and of O_2/Ar pulses (out of 100) are shown.

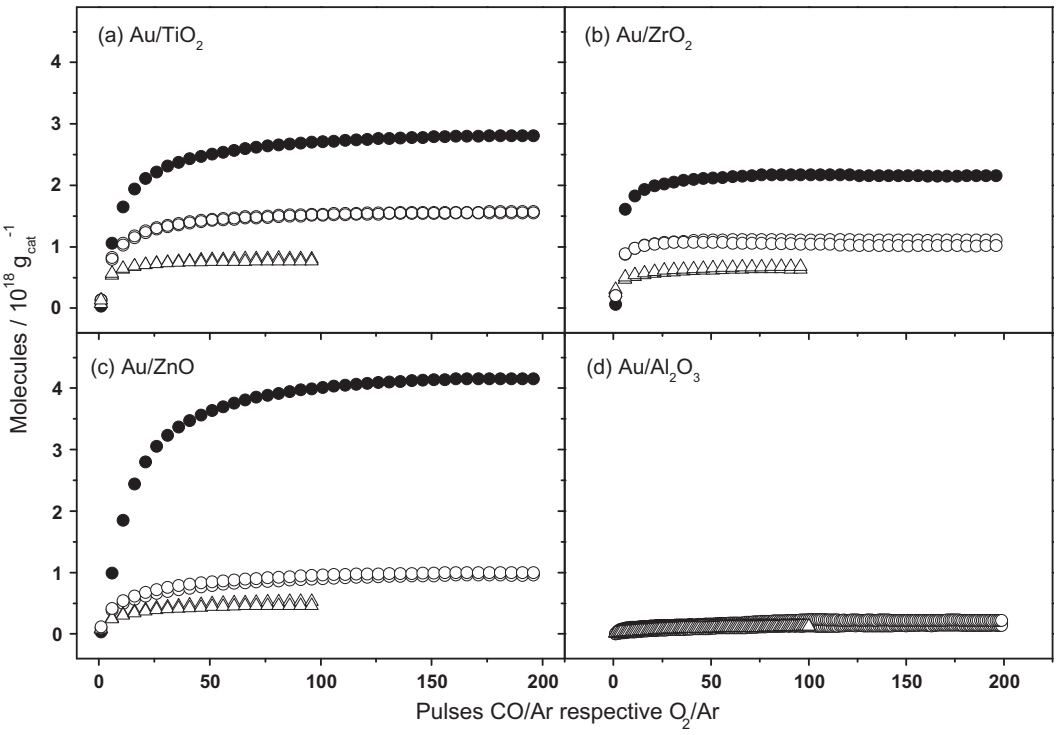

Fig. 5. Total amounts of CO (first sequence: ●; following sequences: ○) and O_2 (Δ) consumed during the multi-pulse experiments on the four differently supported Au catalysts after calcination (10% O_2/N_2, 250 °C, 2 h – O250).

on Au/TiO_2 catalysts based on porous and non-porous TiO_2 after calcination at 400 °C. The amounts of additionally consumed surface oxygen during the first sequence of CO pulses, which reflects the additional amount of oxygen deposited during O250 pre-treatment compared to deposition during re-oxidation by O_2 pulsing at 120 °C, differ for the different catalysts. They are 1.2×10^{18}, 1.1×10^{18}, and 3.2×10^{18} O atoms g_{cat}^{-1} for the Au/TiO_2, Au/ZrO_2, and Au/ZnO catalysts, respectively, and at the limit for quantification (<0.2×10^{18} O atoms g_{cat}^{-1}) for the Au/Al_2O_3 catalyst. After this first sequence, the accumulated amounts of CO converted and O_2 adsorbed during two following sequences equal each other, reflecting reversible reduction and oxidation of the catalyst surface. This amount of oxygen, which is reversibly stored on the catalyst and which can be reversibly removed/replenished by sequences of CO pulses or O_2 pulses, respectively, is defined as the oxygen storage capacity (OSC). It is highest for Au/TiO_2 (1.5×10^{18} O atoms g_{cat}^{-1}) and almost zero for Au/Al_2O_3 (below 0.2×10^{18} O atoms g_{cat}^{-1}). The values for Au/ZnO (0.9×10^{18} O atoms g_{cat}^{-1}) and Au/ZrO_2 (1.2×10^{18} O atoms g_{cat}^{-1}) are in between, with a slightly higher OSC for the latter catalyst (see also Table 2). All samples were measured under identical conditions (pulse size, catalyst bed packing etc.) to enable quantitative comparison.

Because of the similarity in Au loadings, Au particle sizes, and reaction conditions, the differences in the OSC must be related to the different support materials and their ability to reversibly release and store active oxygen, either via adsorption/desorption of oxygen species or via incorporation in and release from the surface lattice. Similar to previous findings [41], the active oxygen stored on the catalysts is only a very small fraction of the total amount of the lattice surface oxygen present on the respective samples. It is about 0.3% for the Au/TiO_2 catalysts under these conditions, in good agreement with recent findings for a P25-supported Au/TiO_2 catalyst (1%) [33], considering the different Au loadings of 1 wt.% and 3.4 wt.%. Since the OSC is even lower for the other catalysts and at the same time their surface areas are comparable (Au/ZnO) or even by a factor of about four higher (Au/ZrO_2 and Au/Al_2O_3), the relative amounts of active surface oxygen stored reversibly on the other catalyst surfaces are even lower, with 0.2% for the Au/ZnO, 0.1% for the Au/ZrO_2, and well below 0.1% for the Au/Al_2O_3 catalyst, respectively. From these findings, it is obvious that the overall surface area of the oxide support, and hence the overall amount of surface oxygen, is not decisive for the oxygen storage capacity of the corresponding catalysts. Following a recent proposal by Kotobuki et al. for Au/TiO_2 catalysts [33], we suggest that on all of these catalysts oxygen storage takes place at the perimeter sites of the interface between Au nanoparticles and support. The previous proposal was based on the observation that for Au/TiO_2 catalysts with different Au particle sizes but constant Au loading and identical support material (P25), the OSC scaled with the number of Au atoms at the perimeter of the interface between Au particles and TiO_2 support [33].

It is important to realize that these amounts of oxygen stored on the different catalysts cannot be detected by any technique under continuous reaction conditions, since the continuous gas flow in these measurements is too high and therefore the time required to deplete or refill the active oxygen is much too short to resolve the additional initial CO or O_2 consumption [53]. For example, in the activity measurements at atmospheric pressure described in Section 3.2, the gas flow for CO or O_2, respectively, is about 1.6×10^{19} molecules min^{-1} (60 Nml min^{-1}, 1 kPa CO or 1 kPa O_2, respectively). Hence, when using 50 mg of catalyst (normally between 0.5 and 60 mg catalyst were used), it would take between 0.3 s (Au/TiO_2) and <0.025 s (Au/Al_2O_3) CO exposure to remove the reversibly stored oxygen on these catalysts, while the time resolution in the GC measurements is about 17 min (one sample taken every 17 min). For mass spectrometric detection, the time resolution would be significantly better, but also there the time constants of the reactor and detection set-up would prevent the detection of

the active oxygen stored on the catalyst surface. Accordingly, an earlier attempt to detect and quantify the OSC via transient IR measurements had failed [53].

In our previous study, the local coverage of reversibly stored oxygen, at 80 °C reaction temperature and after *ex situ* conditioning at 400 °C, was calculated to be 89% relative to the number of Au atoms at the perimeter of the interface between Au particle and TiO_2 support, assuming hemispherical Au nanoparticles and oxygen atoms as the stored species [33]. Here, the local oxygen coverage in the oxidized Au/TiO_2 catalyst is slightly higher (96%), but of similar order of magnitude, independent of the different Au loading (3.4 wt.% in the previous study, 1.0 wt.% in this study). Therefore, we assume that also for the Au/TiO_2 catalyst used in the present work, the active oxygen is located at the perimeter of the interface between Au particles and oxide support. A similar mechanism is suggested also for the other catalysts. Here, the corresponding local active oxygen coverages are lower, obtaining 39% (Au/ZrO_2), 48% (Au/ZnO), and below the detection limit (uncertainty about 10%) for the Au/Al_2O_3 catalyst.

These trends in OSC and in local oxygen coverage agree well with the results of the activity measurements shown in Fig. 3 and, except for Au/ZrO_2, with expectations based on the reducibility of the oxides. Hence, for these different catalysts, there is a clear correlation between activity, OSC and, by and large, the reducibility of the support material of the different Au catalysts, indicating that (i) the deposition and reactive removal of the active oxygen detected in these measurements is a decisive step in the CO oxidation reaction on these catalysts and that (ii) the OSC of the different catalysts is related to the reducibility of the support. It should be noted that for the pure TiO_2 support we could not detect any active oxygen storage under these experimental conditions, i.e., the OSC is clearly related to the presence of the Au nanoparticles.

3.3.2. Activity measurements

The catalytic activity for CO oxidation under reduced pressure was measured by pulsing O_2/Ar and CO/Ar simultaneously over the calcined catalyst samples ($CO:O_2 = 1:1$) at 120 °C reaction temperature. By comparing the consumption of CO and O_2, reaction-induced changes of the oxidation state of the catalyst surface compared to the state after pre-treatment were monitored [33,41]. Furthermore, the possible accumulation of carbon-containing species on the surface and their stability and dynamic behavior during the reaction were determined from differences between the consumption of CO and the formation of CO_2 (Section 3.3.3).

Prior to the measurements, it was checked that under the conditions used in these experiments the pulse shapes and hence the residence times of the educt gases in the catalyst bed are comparable for the different catalysts, despite of the distinct differences in physical properties such as the surface area. This is important, since the conversion of CO and O_2 depends strongly on the partial pressure and on the time needed for a pulse to propagate completely through the catalyst bed ('contact time') [42]. Fig. 6 shows the signals of the Ar component, normalized to the same height, during the activity measurements over the different catalysts. Obviously, the residence times are comparable for all four catalysts.

A representative example of the pulse responses for CO, O_2, Ar, and CO_2 is given in Fig. 7, which shows the respective mass spectrometric responses during 100 simultaneous pulses of CO/Ar and O_2/Ar over the Au/ZnO catalyst. It is obvious already from the raw data that the consumption of CO is initially rather high, but decreases rapidly, whereas that of O_2 is almost constant over the whole experiment. The formation of CO_2 is also highest at the beginning of the reaction and decreases afterward, until reaching a steady-state situation. The results of a quantitative evaluation of similar pulse sequences for all four catalysts are presented in

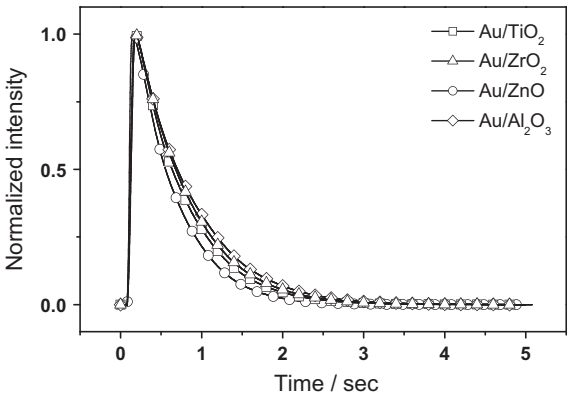

Fig. 6. Pulse shapes of the height-normalized signals of Ar during simultaneous pulses CO/Ar and O_2/Ar for determination of the activity for CO oxidation over the differently supported catalysts after calcination (O250).

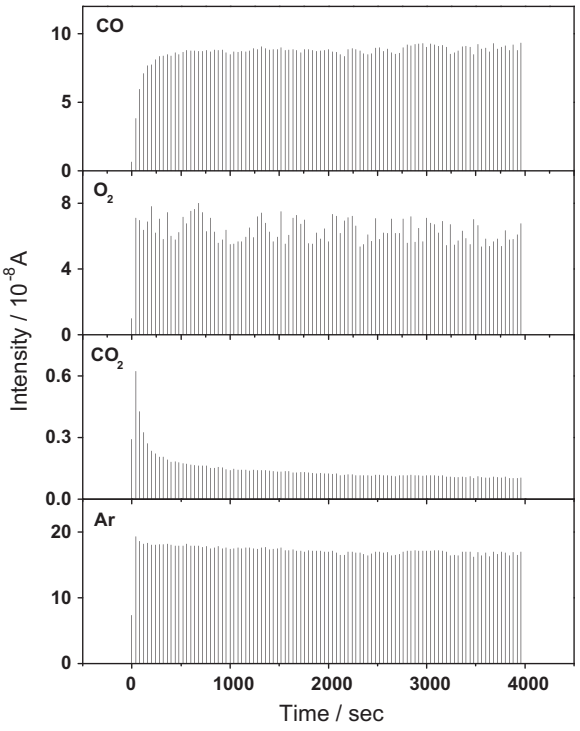

Fig. 7. CO, O_2, CO_2, and Ar signal recorded during a sequence of 100 simultaneous pulses CO/Ar and O_2/Ar dosed on the Au/ZnO catalyst pre-treated by calcination (O250).

Fig. 8, showing the number of CO and O_2 molecules consumed per pulse as well as the number of CO_2 molecules formed. The traces illustrate that for all catalysts, the CO consumption is highest at the beginning and decreases with ongoing pulse number, until reaching constant conversion after about 20–40 pulses. Also the characteristics of the O_2 consumption are similar for all catalysts, starting at almost zero consumption (all O_2 molecules admitted within one pulse exit the reactor) and increasing until reaching steady-state conditions, where stoichiometric consumption of oxygen and CO is achieved. The higher CO consumption compared to the O_2 consumption in the initial period of the reaction over all four catalysts indicates a depletion of active oxygen, equivalent to a reduction of the catalysts after the oxidative pre-treatment. Qualitatively similar observations were reported recently for different Au/TiO_2 catalysts [33,42] and for a Au/CeO_2 catalyst [41].

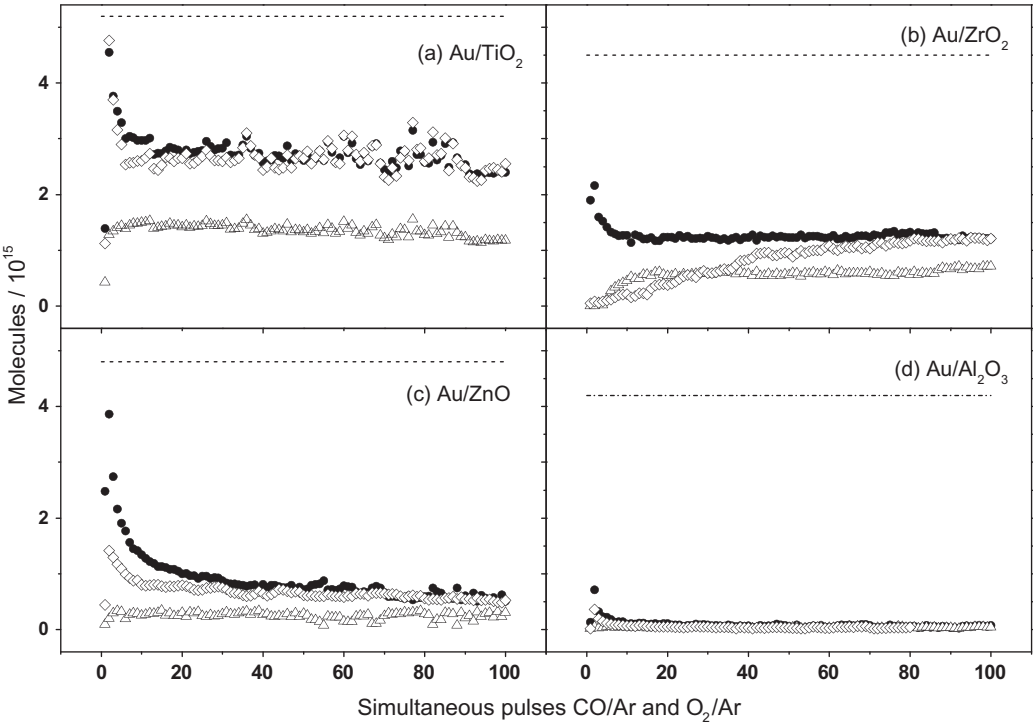

Fig. 8. CO uptake (●), O_2 uptake (△), and CO_2 formation (◇) during admission of simultaneous CO/Ar and O_2/Ar pulses at 120 °C to the differently supported Au catalysts after calcination (O250). The dashed lines indicate the number of consumed CO/produced CO_2 molecules for complete conversion of the CO pulses.

By adding up the differences between CO consumption and O_2 consumption until steady-state is reached with its stoichiometric consumption of CO and O_2, we obtain the absolute amounts of active oxygen removed from the surface during the reaction. These are 1.1×10^{18} O atoms g_{cat}^{-1} for the Au/TiO_2 catalyst, 1.0×10^{18} O atoms g_{cat}^{-1} for Au/ZrO_2, 4.0×10^{18} O atoms g_{cat}^{-1} for Au/ZnO, and below the detection limit for the Au/Al_2O_3 catalyst (see Table 2). We should keep in mind that the single-pulse sequences started on freshly calcined catalyst samples, which have higher amounts of active oxygen on the catalyst surface than after exposure to CO and subsequent re-oxidation by O_2 pulsing in the multi-pulse experiments. The above numbers for active oxygen removal until reaching steady-state are very close to the numbers obtained for the additional active oxygen stored after calcination when compared to the state reached after re-oxidation by O_2 pulsing. Therefore, the steady-state situations during simultaneous CO and O_2 pulses are very close to those obtained after O_2 pulsing alone, and hence the oxidation states of the catalyst surfaces during the mixed pulses are very close to those of the re-oxidized catalysts obtained upon O_2 pulsing.

In contrast to the characteristics of CO and O_2 consumption, that for CO_2 formation differs distinctly between the differently supported catalysts. Furthermore, there are more or less pronounced differences between CO consumption and CO_2 formation, depending on the catalyst (discussion see Section 3.3.3).

For all catalysts, stable reaction conditions with essentially stoichiometric CO and O_2 consumption and equivalent CO_2 formation were reached after 100 pulses. Based on the resulting steady-state conversions, the activities of the different Au catalysts decrease in the order $Au/TiO_2 > Au/ZrO_2 > Au/ZnO > Au/Al_2O_3$, with almost no CO conversion for the Au/Al_2O_3 catalyst. The relative conversions for CO per pulse are 53% for Au/TiO_2, 28% for Au/ZrO_2, 11% for Au/ZnO, and about 2% for Au/Al_2O_3, which is close to the detection limit (see also Table 2). Since the Au content and also the mean Au particle size were almost the same for the different catalysts, also these measurements indicate a pronounced support effect.

The order in activity of the differently supported catalysts in these TAP reactor measurements is similar to that determined in the plug-flow reactor measurements. A quantitative comparison of these two measurements, however, is not possible due to the very different reaction conditions: while we have real steady-state conditions in a continuous flow of gases at atmospheric pressure in the plug-flow reactor measurements, which allow us to calculate reaction rates and TOF numbers, we have a transient input of gases under vacuum conditions in the TAP reactor. Under those conditions, reaction rates are not easily accessible, and we can only calculate the conversion per pulse. Furthermore, the numbers of educt molecules admitted to the catalysts per second and hence their partial pressures are very different in the two measurements. Nevertheless, the fact that the order of the activities is the same in both experiments indicates that at atmospheric pressure the support participates in a similar way in the reaction as in the pulse experiments under low pressure conditions.

Already in 1989, Haruta et al. had proposed that the supporting oxides may play an important role in the CO oxidation over supported Au catalysts, either via metal–support interactions or via a bifunctional mechanism in which gold particle and support oxide activate different steps of the CO oxidation [54]. A distinct effect of the supporting oxide was derived also by Schubert et al., which led them to distinguish between 'active' and 'inert' supports and to tentatively propose sites at the interface between Au nanoparticles and oxide substrate as active sites [29]. In subsequent theoretical studies of the CO oxidation reaction on TiO_2(1 1 0)-supported Au nanorods by Hu and coworkers [30] and by Hammer and coworkers [31], these authors found that molecular O_2 could be stable adsorbed at interface sites, stabilized by interactions with an undercoordinated Au atom and a Ti^{4+} cation, while on Au surfaces the adsorption energy was negligible. Furthermore, this molecular O_2 species was found to be highly activated and able to react with CO adsorbed on the Au nanorod with a rather low reaction barrier of 0.1–0.2 eV [30,31]. Moving onto distinct Au_{10} bilayer clusters supported on rutile TiO_2(1 1 0), Remediakis et al. postulated two

different pathways for the CO oxidation over supported Au catalysts, a 'gold-only mechanism' and a 'metal/oxide boundary mechanism' [32,55]. Their calculations showed stable adsorption of O_2 species both at the interface between the Au_{10} cluster and rutile TiO_2(1 1 0) and also on the Au_{10} cluster, though with different stabilities. Subsequent reaction with CO_{ad} was found to be possible on both sites. In the 'gold-only mechanism', reaction takes place only on the Au nanoparticles, at low-coordinated Au sites such as corners or edges. This mechanism was proposed to be active on all Au catalysts, independent of the support material. Nevertheless, the support can indirectly affect the catalytic performance also in the 'gold-only mechanism' via support-induced modifications of the Au nanoparticles, e.g., via charge transfer or strain effects. In the 'metal/oxide boundary mechanism', oxygen is adsorbed and activated at the interface between Au and the metal oxide support. Due to the charge transfer to the adsorbed O_2 species, this results in negatively charged O_2 species. Such superoxide (and peroxide) species had already been proposed to represent the active oxygen species for CO oxidation by Liu et al. for a Au/Fe_2O_3 catalyst [34]. Furthermore, they were identified on different metal oxide-supported Au catalysts by electron spin resonance (ESR) [56] and Raman spectroscopy measurements [35,57]. The contribution of this pathway depends strongly on the chemical nature of the support, which directly participates in the catalytic reaction. Depending on the reaction conditions, on the preparation and pre-treatment procedure and on the structural and chemical properties of the catalyst (Au particle size, support particle size, and chemical nature of the support), the one or the other pathway was proposed to dominate [32,55].

In a recent quantitative TAP study on the OSC and CO oxidation behavior over P25-supported Au/TiO_2 catalysts with different Au particle sizes but identical Au loading, we found the OSC and also the activity for CO oxidation to scale approximately with the length of the perimeter of the interface between Au nanoparticles and TiO_2 support [33]. This finding provided clear evidence that active oxygen can be adsorbed on sites along the perimeter of the Au–oxide interface. Similar evidence came also from a study of the OSC and CO oxidation behavior on Au/CeO_2 [41]. The nature of the active oxygen species, atomic or molecular oxygen, could not be derived from those measurements. In view of the findings of the theoretical studies described above, which revealed that stable adsorbed molecular oxygen species can be formed at perimeter sites it may be tempting to favor a reaction mechanism proceeding via a molecularly adsorbed O_2 species, as described by the 'metal/oxide boundary mechanism' [32,55]. The atomic O_{ad} species resulting from reaction between CO_{ad} and $O_{2,ad}$ (CO induced $O_{2,ad}$ dissociation) is highly reactive even on extended Au surfaces [58] and also on TiO_2(1 1 0)-supported Au clusters [32,55,59–62] and will react rapidly with coadsorbed CO. On the other hand, however, the observation that the active oxygen species is stable at least up to temperatures of 120 °C is hardly compatible with a molecularly adsorbed oxygen species and with the adsorption energies calculated in theoretical studies [55]. According to calculations by Laursen and Linic [62], atomic oxygen species are most stable bound at the Au/TiO_2 interface, while other sites on the Au nanostructure (2-layer-thick Au nanorods on TiO_2(1 1 0)) may be available for CO adsorption. It should be noted that atomically adsorbed oxygen on Au or Au model catalysts has been demonstrated previously to be highly reactive toward CO [58–60]. On the other hand, the most important open question, the reaction pathway for O_2 dissociation, has not been addressed by Laursen and Linic and is still unresolved. Because of the high thermal stability of the active oxygen species, we also favor an atomic species located at the perimeter of the Au/oxide interface as active species.

Considering the clear correlation between OSC and CO oxidation activity in the present measurements illustrated in Fig. 9, we propose that also for the other Au catalysts the activation of oxygen takes place at the perimeter of the Au–oxide interface ('metal/oxide boundary mechanism'), at least in the dominating reaction pathway. Accordingly, the differences in energy levels and barriers in this reaction pathway are responsible for the differing activities of these catalysts. Only for the Au/Al_2O_3 catalyst with its very little OSC, the contribution from the 'gold-only mechanism', which should be of similar order of magnitude for all catalysts investigated, may be dominant.

The correlation between OSC and activity on the one hand and reducibility of the support on the other hand derived in the present study agrees with trends reported earlier [29]. In the latter measurements, however, the similarity in Au particle size and composition (Au^0) and Au loading of the different catalysts was much less well controlled than in the present study.

The reducibility of the support may affect the catalyst and its performance in different ways. Oxygen vacancy defects were speculated to improve O_2 adsorption on the support or at the support–oxide interface [63,64] or to change the charge state of the Au nanoparticles [49]. In previous calculations, oxygen vacancies at the interface were found to significantly enhance the interaction between oxide and Au nanoparticles, e.g., for $Au–TiO_2$ [65,66] or for Au–MgO [31,36,67]. On the other hand, the effect on the adsorption energies and reaction barriers was found to be rather small [32,55]. Alternatively, the stronger interaction of O_2 with highly charged cations such as Ti^{4+} was held responsible for the high activity of Au catalysts supported on reducible oxides such as TiO_2 or V_2O_5 [30]. Experimentally, Carretin et al. found that upon doping the supporting TiO_2 with iron, the concentration of oxygen vacancies, as estimated from the band-gap transition of TiO_2 in UV–VIS spectra, the number of adsorbed superoxide and peroxide species after O_2 exposure (Raman spectroscopy) and the catalytic activity for CO oxidation increased [35]. In the present experiments, surface oxygen vacancies may be generated during CO pulsing, though definite proof cannot be given. During reaction, after reaching steady-state conditions, however, the catalyst surface was determined to be in a state close to the 'fully oxidized state', where the existence of significant amounts of oxygen vacancies is unlikely.

In total, these experiments clearly support a CO oxidation reaction mechanism involving direct participation of the support ('metal/oxide boundary mechanism'). Despite of the evidence in previous theoretical work, where mainly stable adsorbed molecular O_2 species were found at interface perimeter sites, we tend to favor an atomic species adsorbed at the perimeter of the Au–oxide

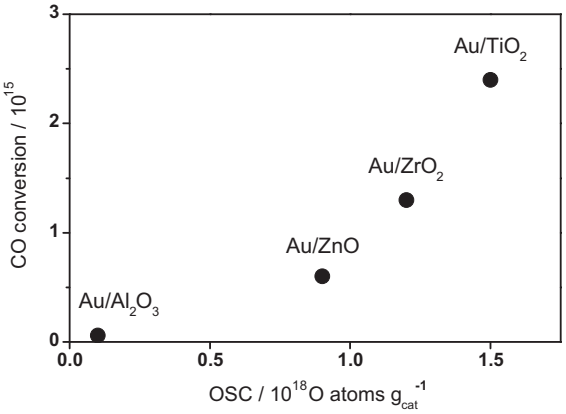

Fig. 9. Absolute amounts of CO converted/CO_2 produced in steady-state during simultaneous pulses CO/Ar and O_2/Ar on the differently supported Au catalysts plotted against the oxygen storage capacity of the corresponding catalysts, both after pre-treatment by calcination (O250).

interface as active oxygen species because of its high stability determined experimentally, being stable toward desorption at least up to 120 °C. Final proof, however, is still missing. The presence of significant amounts of oxygen vacancies during reaction, under steady-state conditions, is unlikely, though it cannot be fully ruled out.

3.3.3. Accumulation of carbon-containing surface species

It is well known from previous studies that carbon-containing surface species are built up on oxide-supported catalysts during CO oxidation [3,68–70]. Depending on the nature of the support, these species may either be stable adsorbed surface species such as surface carbonates, acting as reaction intermediates or spectator species, and/or re-adsorbed product CO_2. Using the TAP reactor, it is possible to exactly quantify the amount of these species, although their nature cannot be identified.

For the more active catalysts investigated, we found a clear difference between CO consumption and CO_2 formation in the single-pulse experiments in the initial phase of the reaction. The discrepancy between CO consumption and CO_2 formation, however, varies distinctly for the different catalysts. While for most catalysts, the amount of gaseous CO_2 product reaches its highest value within the first two pulses and decreases with ongoing pulse number, it increases steadily during the entire experiment for the Au/ZrO_2 catalyst. At the same time, the consumption of CO decreases for all catalysts in the initial period of the reaction, until reaching a steady-state. The number of pulses required for reaching a stable situation with similar values for CO consumption and CO_2 formation differs for the different catalysts. While this is essentially reached after only 2 pulses for the Au/TiO_2 catalyst, it takes about 50 pulses for the Au/ZnO catalyst and almost 100 pulses for the Au/ZrO_2 catalyst. Due to the very low amount of CO consumption and CO_2 formation on the Au/Al_2O_3 catalyst, the time for reaching steady-state could not be determined for this catalyst. These results clearly indicate that some kind of carbon-containing species is formed on the catalyst surface during the reaction, either stable compounds such as surface carbonates, which are built up during reaction or by re-adsorption of the product CO_2. Adding up the differences between CO consumption and CO_2 formation, we calculated the number of carbon-containing surface species formed during the reaction to be equivalent to $<2.0 \times 10^{17}$, 7.7×10^{18}, and 2.7×10^{18} CO_2 molecules g_{cat}^{-1} for the Au/TiO_2, Au/ZrO_2, and Au/ZnO catalyst, respectively (see Table 2). For the Au/Al_2O_3 catalyst, a quantitative evaluation was not possible due to the very low values for CO consumption and CO_2 formation. One should note that there is no correlation between the additional amount of active oxygen present on the catalysts surface after O250 treatment, as indicated by the difference in CO consumption and O_2 consumption, and the formation of adsorbed carbon-containing species, as indicated by the difference in CO consumption and CO_2 formation (for comparison of absolute numbers see Table 2). Therefore, these two effects are discussed separately.

The accumulation of carbon-containing surface species was verified by TPD measurements, performed directly (5 min) after the single-pulse CO oxidation sequences. To distinguish the carbon-containing species from those already present before the reaction, we used labeled ^{13}CO for the single-pulse measurements. The mass 45 TPD traces ($^{13}CO_2$) resulting from the Au/TiO_2, Au/ZnO, and Au/ZrO_2 catalysts (Au/Al_2O_3 was not measured because of the very low CO_2 formation) during these measurements are plotted in Fig. 10a. First of all, although we could not quantify the results of these measurements on an absolute scale, the data clearly reveal a decreasing amount of carbon-containing species in the order Au/ZrO_2 > Au/ZnO > Au/TiO_2, confirming the trend determined in the single-pulse experiments. Second, these spectra exhibit characteristic peaks at about 200–235 °C and 330–360 °C. Recently, Clark et al. proposed for CO oxidation over a Au/TiO_2 catalyst that the interaction of CO_2 product molecules with the support may lead to the transient formation of surface carbonates [53]. These species should decompose slowly to CO_2 which then may re-adsorb again. Based on these results, we attribute the first peak to desorption of adsorbed CO_2, while the second one is tentatively assigned to the decomposition of surface carbonates. The tendency for CO_2 adsorption is low for Au/TiO_2, despite of its high activity for CO_2 formation, slightly higher for Au/ZnO and clearly most pronounced for Au/ZrO_2, where this is the dominant carbon-containing surface species present on the surface during/after reaction. On the other hand, for Au/ZnO, the second peak dominates and it is even higher than that on Au/ZrO_2, where also considerable amounts of these species were formed, while for Au/TiO_2 also this peak has a very low intensity. Hence, on Au/ZnO and in particular on Au/ZrO_2, CO_2 is accumulated by re-adsorption in the catalyst (desorption ~235 °C). In addition, more stable surface compound species are formed (decomposition at 330–360 °C), and here the amount of these species is highest for Au/ZnO species, lower for Au/ZrO_2, and much lower for Au/TiO_2.

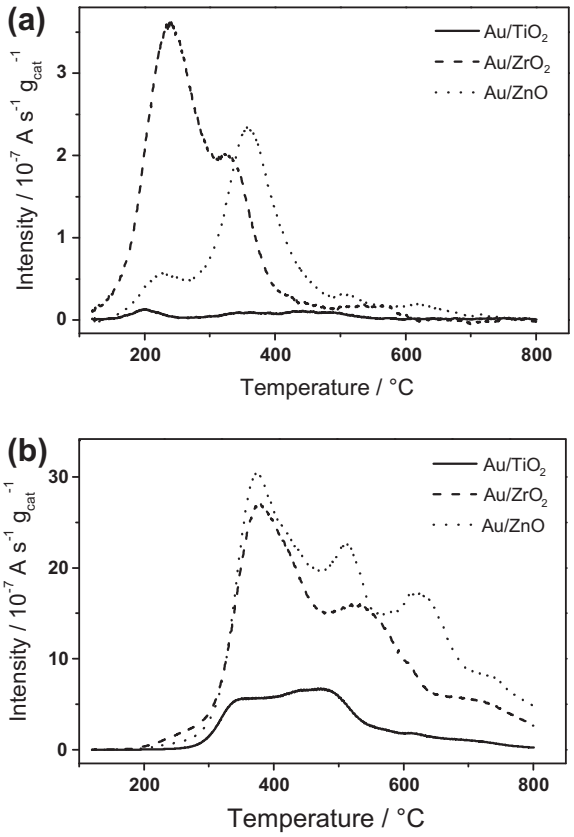

Fig. 10. Mass spectrometric signals for (a) mass 45 ($^{13}CO_2$) and (b) mass 44 ($^{12}CO_2$) recorded during temperature-programmed desorption (TPD) directly after reaction with $^{13}CO/O_2/Ar$ pulses over the Au/TiO_2, Au/ZrO_2, and Au/ZnO catalysts at 120 °C after calcination (O250).

In addition to these species, there are considerable amounts of other stable carbon-containing species on the surface, which were not removed by the pre-treatment procedure. This is evident from the TPD traces recorded on mass 44 ($^{12}CO_2$) during the same TPD measurements over the three catalysts (Fig. 10b). Since the pre-treatment involved calcination at 250 °C, measurable desorption occurs only above that temperature. The data reveal distinct differences in the desorption characteristics between the different catalysts. Also here, the amount of carbon-containing surface species is much higher for the Au/ZnO and Au/ZrO_2 catalysts than for the Au/

TiO_2 catalyst, in line with the activities for forming such species described above (Fig. 10a). Furthermore, we find a characteristic peak or shoulder at about 350–375 °C, which may result from the same surface species as the high temperature peak in Fig. 10a, plus a number of higher temperature peaks which are likely to be related to other surface species.

The stability and dynamic behavior of the carbon-containing surface species on the three catalysts during the reaction was explored by isotope switching experiments (for Au/Al_2O_3, this was not done because of the low activity for CO_2 formation and hence for the low build-up of carbon-containing deposits). We first admitted 50 pulses of a gas mixture of labeled ^{13}CO, O_2, and Ar to the freshly calcined catalysts, and then changed to 50 pulses of ^{12}CO, O_2, and Ar. The CO and O_2 conversions and the formation of the two CO_2 isotopomers ($^{13}CO_2$, $^{12}CO_2$) are shown in Fig. 11. On the Au/TiO_2 catalyst, there is almost no build-up of carbon-containing surface species at the beginning (see also above), and the small amount of reversibly stored carbon-containing surface species present during reaction is exchanged completely within the first 5 pulses after the switch (100% exchange). This is in good agreement with expectations based on a weak interaction between CO_2 and TiO_2. The situation is very different for the Au/ZrO_2 and the Au/ZnO catalysts. On these catalysts, one can detect isotope-labeled $^{13}CO_2$ molecules even 50 pulses after the switch to ^{12}CO. Correspondingly, the intensity of the new $^{12}CO_2$ isotopomer increases only slowly and has not yet reached its final value even after 50 pulses. Until the end of the sequence, only part of the ^{13}C carbon-containing surface species accumulated during the preceding reaction sequence were replaced by their ^{12}C analogs (57% for Au/ZrO_2 and 29% for Au/ZnO). From the fact that $^{13}CO_2$ formation is not observed continuously, as one would expect from thermal desorption, but only upon $^{12}CO/O_2$ pulses, we can further conclude that the replacement of adsorbed ^{13}C species by ^{12}C species on the surface is essentially induced by CO_2 rather than just due to thermal desorption of CO_2. The third possibility, CO or O_2 induced decomposition, could be excluded by additional pulse experiments using CO or O_2 pulses only. The observation of a slow exchange of the carbon-containing species during reaction over the Au/ZrO_2 and the Au/ZnO catalysts is consistent with the thermal stability of these species detected in the TPD measurements (desorption maxima at 200–235 °C and at 330–360 °C). Most likely, mainly the species in the low-temperature peak (re-adsorbed CO_2) are exchanged. Considering the relative amounts of exchanged species, however, the exchange must involve also the high temperature species (stable surface carbonate species), at least for Au/ZnO, though presumably on a slower time scale.

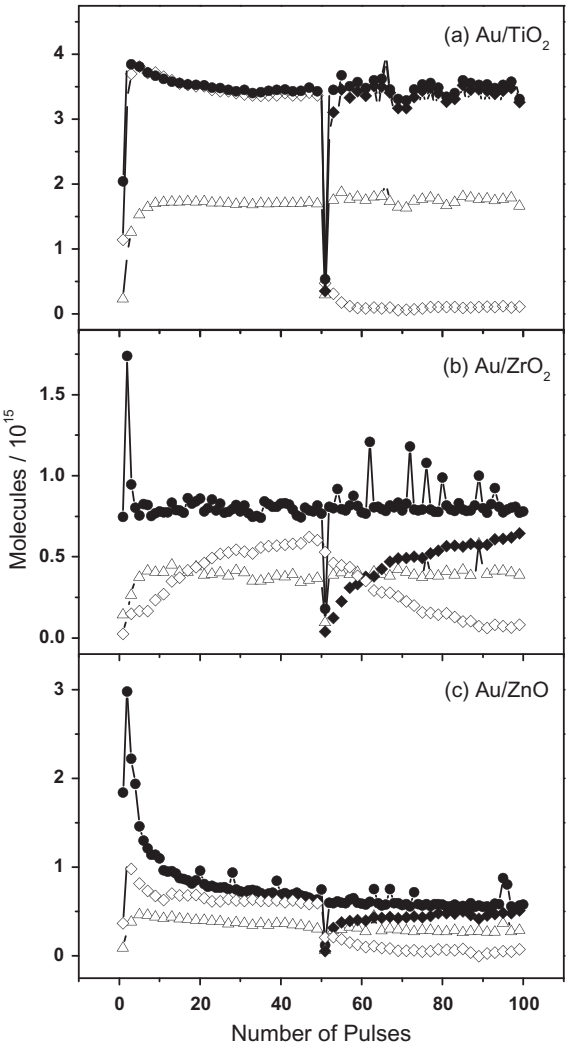

Fig. 11. CO uptake (●), O_2 uptake (Δ), and CO_2 formation (◇: open symbols $^{13}CO_2$, filled symbols $^{12}CO_2$) per pulse during isotope switching experiments at 120 °C, exposing the freshly calcined (O250) (a) Au/TiO_2, (b) Au/ZrO_2, and (c) Au/ZnO catalysts first to 50 $^{13}CO/O_2/Ar$ pulses and afterward to 50 $^{12}CO/O_2/Ar$ pulses. (Instabilities in the O_2 pulses were corrected for in the quantitative evaluation by comparison with the Ar standard.)

The presence of significant amounts of carbon-containing species on the surface, also at the beginning of the reaction, and the very different tendencies for further deposition of these species during the reaction may be another factor affecting the (initial) activity of these Au catalysts, in addition to their different inherent activities (activity of a catalyst free of carbon-containing deposits). As shown in previous reaction measurements, increasing coverages of carbon-containing surface species result in a lower activity of the corresponding catalysts [70–73]. Although we expect only a small fraction of these surface species to be located at the active interface perimeter sites, a higher coverage of these species on the support goes along with a higher probability for blocking these interface sites. Therefore, the relatively low coverage of carbon-containing surface species on the Au/TiO_2 catalyst may be further reason for the high activity of this catalyst and may at least partly be responsible for its much higher activity compared to Au/ZrO_2, despite the rather small difference in OSC (factor of 1.2). Moreover, the weak interaction between CO_2 and the TiO_2 support can also explain the extraordinary high activity of Au/TiO_2 catalysts already at very low temperatures (−70 °C), which has been reported previously [3]. On other, more strongly interacting support materials, adsorption of CO_2, and accumulation of carbon-containing surface species would lead to a rapid blocking of surface sites and hence to deactivation. Finally, we want to note that due to the very different reaction times the build-up of carbon-containing surface species sensed in the TAP reactor measurements cannot be compared, at least not quantitatively, with the deactivation detected in microreactor measurements (Fig. 3 and [70]). On time scales of hours and more, as used in such experiments, carbon-containing surface species are built up also on Au/TiO_2 and lead to a significant deactivation of the catalyst, in particular at lower temperatures (80 °C) [70,73].

4. Conclusions

Applying quantitative Temporal Analysis of Products techniques, we could quantify the oxygen storage capacity (OSC) of four Au catalysts supported on different oxide materials but with

similar Au loadings and Au particle sizes and relate this to the catalytic activity for CO oxidation reaction. This way we could demonstrate that both OSC and CO oxidation activity depend sensitively and directly on the nature of the support. These measurements in combination with reaction rate and TPD measurements led to the following conclusions:

(1) From the pronounced effect of the support material on the OSC and the activity for CO oxidation and the close correlation between OSC and CO oxidation activity, with the same order in both cases (Au/TiO_2 > Au/ZrO_2 > Au/ZnO > Au/Al_2O_3), we propose a similar reaction mechanism for these catalysts as derived recently for Au/TiO_2 [33], with the support participating directly in the CO oxidation reaction, by stabilizing and activating adsorbed oxygen at the perimeter sites of the interface between Au nanoparticle and support ('metal/oxide boundary mechanism'). The data clearly suggest that the reactivity is largely controlled by the OSC of the catalyst. Only for the Au/Al_2O_3 catalyst with its very low OSC and CO oxidation activity, the reaction may be dominated by a 'gold-only mechanism'.

(2) From the pronounced effects of the support and the similar order of decreasing activity obtained in stationary measurements of the reaction rate in a plug-flow reactor, we conclude that this reaction mechanism is not only dominant under the instationary reaction conditions present in the TAP reactor but also under stationary reaction conditions at atmospheric pressure. Correspondingly, the active oxygen species determined in the pulse experiments is also the active species during continuous oxidation at atmospheric pressure.

(3) From the fact that the surface of all catalysts was essentially in the 'fully oxidized' state during steady-state CO oxidation as obtained upon re-oxidation by O_2 pulsing, we conclude that during reaction contributions from surface vacancies are small, at least under present reaction conditions. More significant, the chemical nature of the support may affect the reaction also via an enhanced formation and stabilization of active oxygen species adsorbed at the interface perimeter sites, by interaction with highly loaded cations such as Ti^{4+} [30].

(4) The distinct differences between the Au catalysts in the tendency for accumulation of carbon-containing surface species during CO oxidation, by re-adsorption of CO_2 product molecules and by formation of stable adsorbed surface species such as surface carbonates, are likely to represent another important factor for the CO oxidation activity of oxide-supported Au catalysts, in addition to the differences in the OSC. Furthermore, the little interaction between CO_2 and Au/TiO_2 catalyst is held responsible for its high activity at low temperatures, where for other Au catalysts the surface would rapidly be covered by adsorbed CO_2 and surface carbonates, etc.

(5) From the observation that the adsorbed carbon-containing species can be reversibly re-converted into CO_2 upon exposure to CO/O_2 mixtures, which was detected in pulse experiments using isotope-labeled ^{13}CO, we conclude that these species are not fully stable at the reaction temperature, but can be desorbed/decomposed. Since thermal desorption/decomposition of these species occurs only at significantly higher temperatures, this is attributed to a CO_2-assisted mechanism. Because of the rather slow exchange process, we propose that they essentially represent spectator species, which can be formed and decomposed reversibly during the reaction, rather than reaction intermediates in the dominant reaction pathway.

In total, these experiments and results provide definite proof for a direct participation of the support in the CO oxidation reaction over highly active Au/TiO_2, $AuZrO_2$, Au/ZnO catalysts, via activation and storage of active oxygen. Based on previous results for Au/TiO_2, this occurs most likely at the perimeter of the Au–support interface ('metal/oxide boundary mechanism'). For Au/Al_2O_3, such participation of the interface cannot be identified, and a 'gold-only mechanism', which at most represents a minority pathway on the other catalysts, may be dominant. We suggest that, in addition to the CO oxidation reaction, these results and findings are important also in a more general sense, for the mechanistic understanding of oxidation reactions over oxide-supported Au catalysts in general, where the same active oxygen species are expected to participate in the reaction.

Acknowledgment

This work was supported by the Deutsche Forschungsgemeinschaft in the Priority Program 1181 (project Be 1201/13-3).

References

[1] G.C. Bond, C. Louis, D.T. Thompson, in: Catalysis by Gold, Imperial Press, London, 2007. Chapter 6.
[2] M. Haruta, T. Kobayashi, H. Sano, N. Yamada, Chem. Lett. 16 (1987) 405.
[3] M. Haruta, S. Tsubota, T. Kobayashi, H. Kageyama, M.J. Genet, B. Delmon, J. Catal. 144 (1993) 175.
[4] G.J. Hutchings, Gold Bull. 29 (1996) 123.
[5] G.C. Bond, D.T. Thompson, Catal. Rev. Sci. Eng. 41 (1999) 319.
[6] Q. Fu, H. Saltsburg, M. Flytzani-Stephanopoulos, Science 301 (2003) 935.
[7] G. Jacobs, P.M. Patterson, L. Williams, D. Sparks, H. Davis, Catal. Lett. 96 (2004) 97.
[8] R. Burch, Phys. Chem. Chem. Phys. 8 (2006) 5483.
[9] W. Deng, M. Flytzani-Stephanopoulos, Angew. Chem. 118 (2006) 2343.
[10] M. Haruta, Catal. Surv. Jpn. 1 (1997) 61.
[11] T. Hayashi, K. Tanaka, M. Haruta, J. Catal. 178 (1998) 566.
[12] R.J.H. Grisel, B.E. Nieuwenhuys, Catal. Today 64 (2001) 69.
[13] M.C. Kung, R.J. Davis, H.H. Kung, J. Phys. Chem. C 111 (2007) 11767.
[14] T.V.W. Janssens, B.S. Clausen, B. Hvolbaek, H. Falsig, C.H. Christensen, T. Bligaard, J.K. Nørskov, Top. Catal. 44 (2007) 15.
[15] M. Haruta, Catal. Today 36 (1997) 153.
[16] M. Valden, X. Lai, D.W. Goodman, Science 281 (1998) 1647.
[17] J.-D. Grunwaldt, M. Maciejewski, O.S. Becker, P. Fabrizioli, A. Baiker, J. Catal. 186 (1999) 458.
[18] M. Mavrikakis, P. Stoltze, J.K. Nørskov, Catal. Lett. 64 (2000) 101.
[19] Z.-P. Liu, P. Hu, A. Alavi, J. Am. Chem. Soc. 124 (2002) 14770.
[20] L.M. Molina, B. Hammer, Phys. Rev. Lett. 90 (2003) 206102.
[21] N. Lopez, T.V.W. Janssens, B.S. Clausen, Y. Xu, M. Mavrikakis, T. Bligaard, J.K. Nørskov, J. Catal. 223 (2004) 232.
[22] T.V.W. Janssens, A. Carlsson, A. Puig-Molina, B.S. Clausen, J. Catal. 240 (2006) 108.
[23] S.H. Overbury, V. Schwartz, D.R. Mullins, W. Yan, S. Dai, J. Catal. 241 (2006) 56.
[24] E.D. Park, J.S. Lee, J. Catal. 186 (1999) 1.
[25] R.M. Finch, N.A. Hodge, G.J. Hutchings, A. Meagher, Q. Pankhurst, M.R.H. Siddiqui, F.E. Wagner, R. Whyman, Phys. Chem. Chem. Phys. 1 (1999) 485.
[26] J.C. Fierro-Gonzalez, B.C. Gates, J. Phys. Chem. B 108 (2004) 16999.
[27] J.A. van Bokhoven, C. Louis, J.T. Miller, M. Tromp, O.V. Safonova, P. Glatzel, Angew. Chem. Int. Ed. 45 (2006) 4651.
[28] L. Delannoy, N. Weiher, N. Tsapatsaris, A.M. Bessley, L. Ncharib, S.L.M. Schroeder, C. Louis, Top. Catal. 44 (2007) 263.
[29] M.M. Schubert, S. Hackenberg, A.C. van Veen, M. Muhler, V. Plzak, R.J. Behm, J. Catal. 197 (2001) 113.
[30] Z.-P. Liu, X.-Q. Gong, J. Kohanoff, C. Sanchez, P. Hu, Phys. Rev. Lett. 91 (2003) 266102.
[31] L.M. Molina, M.D. Rasmussen, B. Hammer, J. Chem. Phys. 120 (2004) 7673.
[32] I.N. Remediakis, N. Lopez, J.K. Nørskov, Appl. Catal. A 291 (2005) 13.
[33] M. Kotobuki, R. Leppelt, D. Hansgen, D. Widmann, R.J. Behm, J. Catal. 264 (2009) 67.
[34] H. Liu, A.I. Kozlov, A.P. Kozlova, T. Shido, Y. Iwasawa, Phys. Chem. Chem. Phys. 1 (1999) 2851.
[35] S. Carrettin, Y. Hao, V. Aguilar-Guerrero, B.C. Gates, S. Trasobares, J.J. Calvino, A. Corma, Chem. Eur. J. 13 (2007) 7771.
[36] A. Sanchez, S. Abbet, U. Heiz, W.-D. Schneider, H. Häkkinen, R.N. Barnett, U. Landman, J. Phys. Chem. A 102 (1999) 9573.
[37] C.K. Costello, M.C. Kung, H.-S. Oh, Y. Wang, H.H. Kung, Appl. Catal. A 232 (2002) 159.
[38] J.-D. Grunwaldt, C. Kiener, C. Wögerbauer, A. Baiker, J. Catal. 181 (1999) 223.
[39] S. Arrii, F. Morfin, A.J. Renouprez, J.L. Rousset, J. Am. Chem. Soc. 126 (2004) 1199.

[40] M. Comotti, W.-C. Li, B. Spliethoff, F. Schüth, J. Am. Chem. Soc. 128 (2006) 917.
[41] D. Widmann, R. Leppelt, R.J. Behm, J. Catal. 251 (2007) 437.
[42] A. Tost, D. Widmann, R.J. Behm, J. Catal. 266 (2009) 299.
[43] S. Biella, F. Porta, L. Prati, M. Rossi, Catal. Lett. 90 (2003) 23.
[44] M. Comotti, C. Pina, R. Matarrese, M. Rossi, A. Siani, Appl. Catal. A 291 (2005) 204.
[45] M.J. Kahlich, H.A. Gasteiger, R.J. Behm, J. Catal. 171 (1997) 93.
[46] R. Leppelt, D. Hansgen, D. Widmann, T. Häring, G. Bräth, R.J. Behm, Rev. Sci. Instrum. 78 (2007) 104103.
[47] J.T. Gleaves, G.S. Yablonskii, P. Phanawadee, Y. Schuurman, Appl. Catal. A 160 (1997) 55.
[48] S.O. Shekhtman, G.S. Yablonsky, S. Chen, J.T. Gleaves, Chem. Eng. Sci. 54 (1999) 4371.
[49] G.C. Bond, D.T. Thompson, Gold Bull. 33 (2000) 41.
[50] M.C. Kung, C. Costello, H.H. Kung, Catalysis 17 (2004) 152.
[51] A. Wolf, F. Schüth, Appl. Catal. A 226 (2002) 1.
[52] N. Weiher, E. Bus, L. Delannoy, C. Louis, D.E. Ramaker, J.T. Miller, J.A. van Bokhoven, J. Catal. 240 (2006) 100.
[53] J.C. Clark, S. Dai, S.H. Overbury, Catal. Today 126 (2007) 135.
[54] M. Haruta, N. Yamada, T. Kobayashi, S. Iijima, J. Catal. 115 (1989) 301.
[55] I.N. Remediakis, N. Lopez, J.K. Nørskov, Angew. Chem. 117 (2005) 1858.
[56] Z. Hao, L. Fen, G.Q. Lu, J. Liu, L. An, H. Wang, Appl. Catal. A 213 (2001) 173.
[57] J. Guzman, S. Carrettin, A. Corma, J. Am. Chem. Soc. 127 (2005) 3286.
[58] J.M. Gottfried, K. Christmann, Surf. Sci. 566–568 (2004) 1112.
[59] T.S. Kim, J.D. Stiehl, C.T. Reeves, R.J. Meyer, C.B. Mullins, J. Am. Chem. Soc. 125 (2003) 2018.
[60] J.D. Stiehl, T.S. Kim, C.T. Reeves, R.J. Meyer, C.B. Mullins, J. Phys. Chem. B 108 (2004) 7917.
[61] J.G. Wang, B. Hammer, Phys. Rev. Lett. 97 (2006) 136107.
[62] S. Laursen, S. Linic, Phys. Chem. Chem. Phys. 11 (2009) 11006.
[63] F. Boccuzzi, A. Chiorini, M. Manzoli, P. Lu, T. Akita, S. Ichikawa, M. Haruta, J. Catal. 202 (2001) 256.
[64] M. Manzoli, A. Chiorino, F. Boccuzzi, Surf. Sci. 532–535 (2003) 377.
[65] E. Wahlström, N. Lopez, R. Schaub, P. Thostrup, A. Rønnau, C. Africh, E. Laegsgaard, J.K. Nørskov, F. Besenbacher, Phys. Rev. Lett. 90 (2003) 026101.
[66] N. Lopez, J.K. Nørskov, T.V.W. Janssens, A. Carlsson, A. Puig-Molina, B.S. Clausen, J.-D. Grunwaldt, J. Catal. 225 (2004) 86.
[67] B. Yoon, H. Häkkinen, U. Landman, A.S. Wörz, M. Antonietti, S. Abbet, K. Judai, U. Heiz, Science 307 (2005) 403.
[68] M.A. Bollinger, M.A. Vannice, Appl. Catal. B 8 (1996) 417.
[69] F. Boccuzzi, A. Chiorino, S. Tsubota, M. Haruta, J. Phys. Chem. 100 (1996) 3625.
[70] B. Schumacher, Y. Denkwitz, V. Plzak, M. Kinne, R.J. Behm, J. Catal. 224 (2004) 449.
[71] P. Konova, A. Naydenov, Cv. Venkov, D. Mehandjiev, D. Andreeva, T. Tabakova, J. Mol. Catal. A 213 (2004) 235.
[72] P. Konova, A. Naydenov, T.T. Tabakova, D. Mehandjiev, Catal. Commun. 5 (2004) 537.
[73] Y. Denkwitz, B. Schumacher, G. Kucerova, R.J. Behm, J. Catal. 267 (2009) 78.